Published in final edited form as:
Inflamm Bowel Dis. 2010 February ; 16(2): 320–331. doi:10.1002/ibd.21066.

Ablation of Gly96/Immediate Early Gene-X1 (gly96/iex-1) Aggravates DSS-Induced Colitis in Mice: Role for gly96/iex-1 in the Regulation of NF-κB

Christian Sina, MD[#*], **Alexander Arlt, MD**[#†], **Olga Gavrilova, PhD**[*], **Emilie Midtling, MSc**[*], **Marie-Luise Kruse, PhD**[†], **Susanne Sebens Müerköster, PhD**[†], **Rajiv Kumar, PhD, MD**[‡], **Ulrich R. Fölsch, MD**[†], **Stefan Schreiber, MD**[*], **Philip Rosenstiel, MD**[#*], and **Heiner Schäfer, PhD**[#†]

[*]Institute of Clinical Molecular Biology, UKSH-Campus Kiel, Kiel, Germany

[†]Laboratory of Molecular Gastroenterology & Hepatology, Department of General Medicine, UKSH-Campus Kiel, Kiel, Germany

[‡]Departments of Medicine, Biochemistry and Molecular Biology, Mayo Clinic, Rochester, Minnesota.

[#] These authors contributed equally to this work.

Abstract

Background—Inflammatory bowel diseases (IBDs) result from environmental and genetic factors and are characterized by an imbalanced immune response in the gut and deregulated activation of the transcription factor NF-κB. Addressing the potential role of gly96/iex-1 in the regulation of NF-κB in IBD, we used the dextran sodium sulfate (DSS) colitis model in mice in which the *gly96/iex-1* gene had been deleted.

Methods—C57BL/6 mice of *gly96/iex-1*$^{-/-}$ or *gly96/iex-1*$^{+/+}$ genotype were treated continuously with 4% DSS (5 days) and repeatedly with 2% DSS (28 days) for inducing acute and chronic colitis, respectively. In addition to clinical and histological exploration, colon organ culture and bone marrow-derived cells (BMCs) were analyzed for chemo/cytokine expression and NF-κB activation.

Results—Compared to wildtype littermates, *gly96/iex-1*$^{-/-}$ mice exhibited an aggravated phenotype of both acute and chronic colitis, along with a greater loss of body weight and colon length. Colonic endoscopy revealed a higher degree of hyperemia, edema, and bleeding in *gly96/iex-1*$^{-/-}$ mice, and immunohistochemistry detected massive mucosal infiltration of leukocytes and marked histological changes. The expression of proinflammatory chemoand cytokines was higher in the colon of DSS-treated *gly96/iex-1*$^{-/-}$ mice, and the NF-κB activation was enhanced particularly in the distal colon. In cultured BMCs from *gly96/iex-1*$^{-/-}$ mice, Pam_3Cys_4 treatment induced expression of proinflammatory medi ators to a higher degree than in *gly96/iex-1*$^{+/+}$ BMCs, along with greater NF-κB activation.

Conclusions—Based on the observation that genetic ablation of gly96/iex-1 triggers intestinal inflammation in mice, we demonstrate for the first time that gly96/iex-1 exerts strong antiinflammatory activity via its NF-κB-counterregulatory effect.

Reprints: Heiner Schäfer, PhD, Schittenhelmstr. 12, 24105 Kiel, Germany (hschaef@1med.uni-kiel.de).

Additional supporting information may be found in the online version of this article.

Keywords

intestinal inflammation; signal transduction; cytokines; feedback regulation

The transcription factor NF-κB plays a fundamental role in inflammation, cellular stress control, and cellular survival.[1–3] NF-κB controls the expression of antiapoptotic factors and of many genes encoding proinflammatory mediators such as cytokines, adhesion molecules, and chemokines. Deregulated NF-κB activity has been implicated in numerous pathological conditions including malignancies[4] and chronic inflammatory disorders, e.g., rheumatoid arthritis and inflammatory bowel disease (IBD).[5–7] Since NF-κB is activated by a large number of stimuli, tight molecular feedback loops normally prevent sustained cellular responses and excessive inflammation.

NF-κB-induced expression of the major NF-κB inhibitory protein IκBα plays a fundamental role acting as a direct feedback inhibitory system, yet other more subtle feedback inhibitors also exist, i.e., the de-ubiquitinases A20 and CYLD.[2,8,9] We have shown previously that the stress response gene IEX-1,[10] also known as DIF-2/IER3, or the mouse homolog gly96[11,12] represents an NF-κB target gene and serves as a complex feedback inhibitor of NF-κB at multiple cellular levels.[13,14] The 156 amino acids protein displays no sequence homology with other human proteins and is highly conserved among vertebrates.[10,12,15] Multiple functional studies reveal that gly96/iex-1 exerts a dual role in cellular growth control and apoptosis. For example, in epithelial cells, hepatocytes and keratinocytes gly96/iex-1 enhances apoptosis,[16–20] whereas in hematological precursor cells and in immune cells gly96/iex-1 favors cellular survival and differentiation.[21–23] Recent studies have shown that gly96/iex-1 expression is inversely related to the formation of malignant tumors of the colon,[20,24] pancreas,[25] and endocrine tissues,[26] thus indicating a tumor-suppressive potential of gly96/iex-1.

Given these complex cellular actions gly96/iex-1 could affect cellular viability through negative interference with NF-κB activation. To some extent this action relies on the dampening of IκBα degradation, thereby leading to a reduced nuclear localization of NF-κB.[14–18] Moreover, in a recent study we showed that gly96/iex-1 is also capable of directly binding to p65/RelA, leading to the inhibition of p65-dependent gene transcription.[13] Thus, gly96/iex-1 is part of a NF-κB/RelA-dependent counterregulatory mechanism that might be particularly relevant to the control of inflammatory responses. This would probably not apply to other NF-κB members, i.e., p50/nfkb1, that have been shown to also exert antiinflammatory activity.[27,28]

Inflammatory bowel disease (IBD) which manifests as either ulcerative colitis (UC) or Crohn's disease (CD), is an archetypal chronic inflammatory disorder caused by a complex interplay of both environmental and genetic factors.[29] Aberrant NF-κB activation, probably caused by exposure to enteric bacteria or genetic alterations, is a hallmark of inflammatory episodes of IBD.[5–7,30,31] IBD is associated with the infiltration of the intestinal lamina propria by mononuclear cells such as macrophages or lymphocytes that overexpress the products of NF-κB target genes, including the proinflammatory cytokines tumor necrosis factor alpha (TNFα), interleukin-1β (IL-1β), and IL-6.[32,33]

Notably, a comparative analysis of the mucosal gene expression profile in IBD and healthy individuals identified gly96/iex-1 among the top 10 differentially expressed genes.[34] This observation prompted us to investigate the impact of the genetic ablation of gly96/iex-1 on murine experimental colitis induced by sodium dextran sulfate (DSS). DSS colitis represents a useful model for studying cellular and molecular mechanisms characteristic of IBD.[35–37]

For this purpose we made use of gly96/iex-1-deficient C57BL/6 mice[38] subjected to short-term and long-term DSS treatment. These treatment regimens induce acute and chronic inflammation in the colonic mucosa, respectively. As a remarkable result, we show that the absence of the *gly96/iex-1* gene severely aggravates acute as well as chronic inflammation in DSS-treated mice. These novel findings provide insight into the pathophysiological role of gly96/iex-1 in in vivo inflammation and emphasize its role in NF-κB counterregulation.

MATERIALS AND METHODS

Animals

gly96/iex-1$^{-/-}$ mice on a C57BL/6 background were used at backcross generation >10.[38] Heterozygous parental mice were intercrossed to yield *gly96/iex-1*$^{-/-}$ and *gly96/iex-1*$^{+/+}$ offspring that were used for the experiments upon reaching an age of 9–10 weeks. Animal experiments were approved by the local committee for animal use. Polymerase chain reaction (PCR)-genotyping was conducted as described.[38]

Colitis induction and Determination of Clinical Scores

For acute colitis induction, *gly96/iex-1*$^{-/-}$ and *gly96/iex-1*$^{+/+}$ sex- and age-matched mice were fed 4% DSS (40 kDa; TdB consultancy; Uppsala, Sweden) dissolved in drinking water ad libitum for 5 days. Control mice had access to untreated water. Body weight, stool consistency, and fecal blood loss (Hemoccult test; Beckman Coulter, Krefeld-Fischeln, Germany) were recorded daily. For induction of chronic colitis, sex- and age-matched mice were fed 2% DSS for 5 days followed by 5 days of untreated drinking water. This cycle was repeated 3 times. Animals that lost more than 25% of their initial body weight during the experiments were sacrificed and excluded from data analysis. A high-resolution mouse video endoscopy system was used (HOPKINS(r) Optik 64019BA; KARL STORZ AIDA(tm)VET) and endoscopic scores were obtained as described.[39]

Histopathological and Immunohistochemical Analyses of Mouse Colon Tissue

Postmortem, the entire colon was excised and a 1-cm segment of the descending colon was fixed in 4% paraformaldehyde. Paraffin sections were cut and stained with hematoxylin/eosin. Five colon rings were obtained from each 1-cm colon segment. Histological scoring was performed in a blinded fashion and displays the combined score (0–6) of inflammatory cell infiltration and tissue damage as described.[40] For immunofluorescence staining, cryosections were fixed in ice-cold acetone (10 min) followed by sequential incubation with blocking reagent (Dako, Wiesbaden, Germany) to eliminate nonspecific background staining. Slides were then incubated (1 h, room temperature) with primary antibodies against CD3 (1:50, Abcam; Cambridge, UK), Ly6G (1:100, Abcam), and F4/80 (1:100, Santa Cruz; Heidelberg, Germany). After washing 3 times with phosphate-buffered saline (PBS), slides were incubated (45 min, room temperature) with Cy3- or FITC-labeled secondary antibodies (Jackson ImmunoResearch; West Grove, PA). Before examination, nuclei were counterstained with DAPI.

Colon Organ Culture

A segment of the distal colon was removed, cut open longitudinally, and washed in PBS containing 100 μg/mL penicillin (Sigma, Deisenhofen, Germany) and 100 μg/mL streptomycin (Sigma). The colon was then further cut into segments of 1 cm^2 and incubated in 24 flat-bottom well culture plates containing 1 mL fresh RPMI 1640 medium supplemented with penicillin and streptomycin at 37°C for 24 hours. Culture supernatants were then harvested and assayed for chemo- and cytokines.

Isolation of Bone Marrow Cells (BMCs)

Bone marrow was isolated from the tibias and femurs of 8–12-week-old mice, then triturated using an 18G needle and passed through a 70-μm nylon mesh cell strainer (Becton Dickinson, Heidelberg, Germany) to make a single cell suspension in DMEM (Biochrom, Berlin, Germany) supplemented with 10 mM Hepes (Invitrogen, Karlsruhe, Germany). BMCs were then counted and resuspended in DMEM at 1×10^6 cells/100 μL. Cells were plated into 12-well plastic cell culture plates at a density of 2×10^6 cells/well in DMEM containing 2 mM L-glutamine (Invitrogen) and penicillin/ streptomycin. The adherent cells obtained after 72 hours were checked by F4/80, CD11b staining for the content of macrophages.

Chemo/cytokine Profiling and Enzyme-linked Immunosorbent Assay (ELISA)

Supernatants from colon organ culture or BMC culture were cleared by centrifugation (6,000 rpm, 5 min, 4°C). Protein concentration was determined by the Dc-protein assay (Bio-Rad, Munich, Germany) and the DNA content of BMCs was quantified. For a qualitative screening for the chemo/cytokine content, colon culture supernatants were adjusted to equal protein concentration and analyzed using mouse cytokine proteome profiler arrays (R&D Systems; Wiesbaden, Germany) following the manufacturer's instructions. Arrays were developed with Super-Signal West Dura solution (Perbio Sciences, Bonn, Germany), analyzed with the Chemidoc-System (Bio-Rad), and normalized to the internal array controls. To quantify chemo/cytokine contents, ELISA using commercially available components (R&D Systems) quantifying murine monocyte chemoattractant protein-1 (MCP-1/JE), murine keratinocyte-derived chemokine (KC), monokine induced by γ-interferon (MIG), IL-1β, and IL-6 were performed following the manufacturer's protocols. Chemo/cytokine concentrations were determined in duplicate and normalized to the protein content of colon culture supernatants or the DNA concentration of BMCs.

Tissue Homogenization

Frozen tissue specimens from colon segments were homogenized (30 sec, 15,000 rpm) using the cryogenic grinding ball mill MM400 (Retsch, Haan, Germany) and submitted to RNA or nuclear extract preparation.

Quantitative RT-PCR

Total RNA was prepared, reverse-transcribed into single-stranded cDNA, and submitted to SYBR-Green real-time PCR as described.[14] IL-6-, KC-, IL-1β-, and MCP-1-primers were from R&D Systems, and mouse bactin-primers from Lonza (Verviers, Belgium). MIG-primers 5′-ACTCAGCTCTGCCATGAAGTCCGC-3′ (sense), 5′-AAAGGCTGCTCTGCCAGGGAAGGC-3′ (antisense) were from Biometra (Göttingen, Germany). PCR conditions are available on request.

Gel-shift Assays

Nuclear extracts were prepared and quality checked as described previously.[41] After adjusting to equal amount of protein, samples were incubated with a γ^{32}P-labeled NF-κB-consensus oligonucleotide (Promega, Mannheim, Germany). After 30 minutes incubation at room temperature, samples were electrophoresed at 100V, 4°C. Gels were dried and exposed to x-ray Hyperfilm (Amersham, Freiburg, Germany).

Western Blot

Cytoplasmic or nuclear extracts were submitted to Western blot as described[18] using primary antibodies against IκBα (Santa Cruz, 1:500) or tubulin (Sigma, 1:2000) incubated overnight at 4°C.

Statistics

Normality of the data was checked by calculating Lilliefors probabilities based on the Kolmogorov–Smirnov test. Results are expressed as means ± SEM. *P*-values were calculated using a multifactorial analysis of variance test and independent *t*-test. *P*-values less than 0.05 were considered statistically significant. Experiments and measurements were replicated at least 3 times.

RESULTS

Higher Disease Activity in DSS-colitis in *gly96/iex-1*$^{-/-}$ Mice

For the induction of acute colitis, mice were treated with 4% DSS (orally, p.o.) for 5 days. Upon DSS treatment, gly96/iex-1-deficient mice exhibited a significantly increased weight loss compared to *gly96/iex-1*$^{+/+}$ mice starting between days 2 and 3 after initiation of DSS administration (Fig. 1A). After 6 days, these animals had already lost 20% of their body weight. In contrast, *gly96/iex-1*$^{+/+}$ mice exhibited a moderate weight loss only after 6 days and the extent of weight loss after 7 days (8%) was significantly lower in comparison with *gly96/iex-1*$^{-/-}$ mice (23%). The severity of disease was also assessed by colon length (Fig. 1B), which was more reduced in DSS-treated *gly96/iex-1*$^{-/-}$ mice (5.9 cm) compared to *gly96/iex-1*$^{+/+}$ mice (–4.8 cm).

Next, mice were subjected to cyclic treatment with 2% DSS (p.o.) for 4 weeks. Under these conditions a chronic colitis developed that, again, was more pronounced in *gly96/iex-1*$^{-/-}$ mice. As shown in Figure 1C, continuous weight loss occurred more progressively in *gly96/iex-1*$^{-/-}$ than in *gly96/iex-1*$^{+/+}$ mice, particularly in the 2–3-day intervals after DSS administration.

At the endpoint after 4 weeks the weight loss was about 20% in *gly96/iex-1*$^{-/-}$ and 10% in *gly96/iex-1*$^{+/+}$ mice. The colon length (Fig. 1D) was again more reduced in *gly96/iex-1*$^{-/-}$ (–3.2 cm) than in *gly96/iex-1*$^{+/+}$ mice (–1.8 cm).

Colon Tissue Architecture Is More Severely Altered upon DSS-colitis in *gly96/iex-1*$^{-/-}$ Mice

While no differences in the macroscopic appearance of the colon were seen under baseline conditions (Fig. 2A, upper panel), colonic endoscopy confirmed the more aggressive course of acute colitis in *gly96/iex-1*$^{-/-}$ mice. As shown in Figure 2A (middle panel), edema, hyperemia, and bloody erosions became evident in the middle to distal colon of 4% DSS-treated *gly96/iex-1*$^{-/-}$ mice, whereas *gly96/iex-1*$^{+/+}$ mice exhibited only moderate edema and hyperemia, and no bloody erosions. Accordingly, the endoscopic scores (Fig. 2B, left panel) increased in 4% DSS-treated *gly96/iex-1*$^{-/-}$ mice (median: 14.5) significantly more than in *gly96/iex-1*$^{+/+}$ mice (median: 10.0). Histological examination of fixed tissue from colon biopsies revealed a marked thickening of the mucosal layer in 4% DSS-treated *gly96/iex-1*$^{-/-}$ mice. As shown in Figure 2C, a massive infiltration of leukocytes into the mucosa and submucosa as well as submucosal edema were seen in the middle to distal colon of *gly96/iex-1*$^{-/-}$ mice. Moreover, loss of crypt structure and eroded surface epithelium were seen in the diseased colons of *gly96/iex-1*$^{-/-}$ mice. In contrast, 4% DSS-treated *gly96/iex-1*$^{+/+}$ mice showed only moderate leukocytic infiltration, no submucosal edema, and partial retention of crypt structures and surface epithelium (Fig. 2C). Accordingly, the

histological score (Fig. 2D, left panel) in 4% DSS-treated *gly96/iex-1*$^{-/-}$ mice (median: 5.3) was significantly higher than in *gly96/iex-1*$^{+/+}$ mice (median: 4.3).

Colonic endoscopy of animals diseased with chronic colitis (Fig. 2A, lower panel and Fig. 2B) revealed only marginal edema and hyperemia (median endoscopic score: 3.5) in *gly96/iex-1*$^{+/+}$ mice, whereas *gly96/iex-1*$^{-/-}$ mice exhibited substantial hyperemia and erosions in the middle to distal colon (median endoscopic score: 10.5). Histological analysis identified a complete change in colonic tissue architecture in 2% DSS-treated *gly96/iex-1*$^{-/-}$ mice characterized by massive leukocyte infiltration penetrating mucosal, submucosal, and muscular layers, as well as by the entire loss of crypt structures and surface epithelium (Fig. 2C). In *gly96/iex-1*$^{+/+}$ mice, infiltrations of leukocytes were moderate and mainly restricted to the submucosal layer, and crypt structures and surface epithelium were partially retained (Fig. 2C). In 2% DSS-treated *gly96/iex-1*$^{-/-}$ mice, the histological score (Fig. 2D, right panel) was again significantly higher (median: 4.8) than in *gly96/iex-1*$^{+/+}$ mice (median: 2.9).

Enhanced Expression of Proinflammatory Chemo/cytokines in *gly96/iex-1*$^{-/-}$ Mice During Acute DSS-colitis

Since the markedly higher disease activity in DSS-treated *gly96/iex-1*$^{-/-}$ mice might relate to an enhanced expression of NF-κB-dependent inflammatory mediators, short-term culture supernatants of distal colon tissue from untreated or 4% DSS-treated *gly96/iex-1*$^{-/-}$ and *gly96/iex-1*$^{+/+}$ mice were analyzed for the secretion of proinflammatory molecules. Using proteome profiling arrays detecting 36 murine chemo/cytokines, an initial screening identified MCP-1/JE and KC as being highly upregulated by 4% DSS treatment in *gly96/iex-1*$^{-/-}$ mice when compared to *gly96/iex-1*$^{+/+}$ mice (Fig. 3A). Other chemo/cytokines were detected by this screening only at moderate levels or appeared to be similarly expressed. As shown by a quantitative ELISA (Fig. 3B), significantly higher levels of MCP-1 (1006 ± 390 versus 342 ± 98 pg/mg protein) and KC (695 ± 257 versus 439 ± 195 pg/mg protein) were detected in the colonic tissue culture from 4% DSS-treated *gly96/iex-1*$^{-/-}$ mice as compared with *gly96/iex-1*$^{+/+}$ mice. To confirm the greater expression of both proinflammatory molecules in 4% DSS-treated *gly96/iex-1*$^{-/-}$ mice, qPCR analysis on RNA samples from colonic tissue was conducted. As shown in Figure 3C, MCP-1 and KC mRNA levels were significantly higher in *gly96/iex-1*$^{-/-}$ than in *gly96/iex-1*$^{+/+}$ mice.

Enhanced Expression of Proinflammatory Chemo/cytokines in *gly96/iex-1*$^{-/-}$ Mice During Chronic DSS-colitis

An analysis of colonic cultures from animals that developed chronic colitis upon 2% DSS treatment over 4 weeks identified a broader panel of proinflammatory molecules secreted to a greater degree in *gly96/iex-1*$^{-/-}$ mice (Fig. 4A). Among these, MCP-1/JE and KC were again found to be more abundant in supernatants from *gly96/iex-1*$^{-/-}$-mouse colonic tissue, and IL-6, IL-1β, and MIG were also elevated. As shown in Figure 4B, ELISA confirmed higher protein levels of MCP-1 (1710 ± 585 versus 1001 ± 406 pg/mg protein), KC (1424 ± 533 versus 903 ± 395 pg/mg protein), IL-6 (2127 ± 926 versus 633 ± 391 pg/mg protein), protein), MIG (120 ± 65 versus 75 ± 36 pg/mg and IL-1β (71 ± 30 versus 50 ± 39 pg/mg protein) in 2% DSS-treated *gly96/iex-1*$^{-/-}$ mice when compared with *gly96/iex-1*$^{+/+}$ mice. qPCR analysis detected a higher induction of MCP-1, KC, IL-6, IL-1β, and MIG mRNA levels in colonic tissues from 2% DSS-treated *gly96/iex-1*$^{-/-}$ mice in comparison with *gly96/iex-1*$^{+/+}$ mice (Fig. 4C).

Activation of NF-κB in Colonic Tissue Is More Pronounced upon DSS Treatment in *gly96/iex-1*$^{-/-}$ Mice

In order to confirm an enhanced NF-κB activity in the more severely inflamed colonic tissue from *gly96/iex-1*$^{-/-}$ mice, samples of distal, middle, and proximal segments of colon from untreated or 2% DSS-treated animals were analyzed by gel shift assay using an NF-κB consensus binding site as radiolabeled probe. As shown in Figure 5A, NF-κB activation observed in tissue from the proximal colon did not differ between *gly96/iex-1*$^{-/-}$ and *gly96/iex-1*$^{+/+}$ mice, whereas in middle and distal colonic tissue NF-κB activation was greater in *gly96/iex-1*$^{-/-}$ than in *gly96/iex-1*$^{+/+}$ mice. This activation pattern fits to distribution of inflammation as well as to distinct expression levels of DSS-induced MCP1 and KC mRNA level which are mainly seen in the distal colon (Suppl. Fig. 3D). Additional gel-shift analyses confirmed the more strongly increased NF-κB activity in distal colon samples from DSS-treated *gly96/iex-1*$^{-/-}$ mice (Fig. 5B,C).

Colonic Mucosa of DSS-treated gly96/iex-1$^{-/-}$ Mice is Infiltrated by Increased Numbers of Macrophages, T-cells, and Neutrophils

To analyze what cell types are contained in the colonic leukocyte infiltrate observed in mice treated with 2% DSS for 4 weeks, immunohistochemical analyses were performed. As shown by CD3-immunofluorescence microscopy, T-lymphocytes were moderately distributed in the colon sections from *gly96/iex-1*$^{+/+}$ mice (18 ± 2 cells/view), whereas CD3+ positive cells were more abundant (35 ± 7 cells/view) in the colon sections from *gly96/iex-1*$^{-/-}$ mice (Fig. 6A). Similarly, F4/80- and Ly6G-immunofluorescence staining (Fig. 6B,C) detected higher numbers of macrophages and neutrophils in the colon sections from *gly96/iex-1*$^{-/-}$ mice (37 ± 5 and 17 ± 2 cells/high-power field-view, respectively) compared to *gly96/iex-1*$^{+/+}$ mice (17 ± 2 and 8 ± 1 cells/high-power field-view, respectively). These data show that the cellular infiltrates in the colonic tissue of DSS-treated *gly96/iex-1*$^{-/-}$ mice are composed of T cells as well as of neutrophils, monocytes, and macrophages, exhibiting not only higher abundance but also a larger area of infiltration.

Induction of Proinflammatory Chemo/cytokines and NF-κB Activation Is Greater in BMCs from *gly96/iex-1*$^{-/-}$ than in BMCs from *gly96/iex-1*$^{+/+}$ Mice

To verify that ablating the gly96/iex-1 gene affects the expression of proinflammatory chemo/cytokines in immune cells, BMCs were isolated from *gly96/iex-1*$^{-/-}$ and *gly96/iex-1*$^{+/+}$ mice and adherent cells were cultured for 72 hours yielding sufficient amounts of macrophages (>30% F4/80,CD11b-positive). This experimental procedure was chosen to keep the duration of the experiment short enough to avoid altered apoptosis effects that could be expected from gly96/iex-1 gene deficiency. As shown by ELISA (Fig. 7A), treatment of BMCs with the selective TLR2 agonist Pam_3Cys_4 (200 ng/mL, 24 hours) led to increased protein level of MCP-1, IL-6, KC, and IL-1b in BMCs of either *gly96/iex-1* genotype. Intriguingly, in *gly96/iex-1*$^{-/-}$ BMCs the protein level of all 4 chemo/cytokines were significantly higher than in *gly96/iex-1*$^{+/+}$ BMCs. qPCR analysis (Fig. 7B) detected higher mRNA levels of MCP-1, IL-6, KC, and IL-1b in Pam_3Cys_4 treated (4 hours) and untreated *gly96/iex-1*$^{-/-}$ BMCs when compared with *gly96/iex-1*$^{+/+}$ BMCs.

Gel-shift assays detected an increased NF-κB activity in Pam_3Cys_4 treated (1 hour) BMCs that was higher in *gly96/iex-1*$^{-/-}$ than in *gly96/iex-1*$^{+/+}$ cells (Fig. 7C). Moreover, the enhanced NF-κB induction in *gly96/iex-1*$^{-/-}$ BMCs relates to an increased turnover rate of IκBα (Fig. 7D), an observation in line with the negative interference of gly96/iex-1 with the degradation of IκBα.[18]

DISCUSSION

Our present study demonstrates for the first time that ablation of the early response gene gly96/iex-1 triggers inflammation in mice in vivo, as shown here through DSS-induced acute or chronic colitis models. Clinical symptoms upon DSS treatment[37] are more severe in mice if the *gly96/iex-1* gene is deleted. The aggravated diseased phenotype reflects many of the clinical signs of fulminant human IBD, particularly body weight loss, diarrhea, intestinal bleeding, extended mucosal damage[42,43] and alterations of intestinal tissue architecture. Accordingly, intestinal expression levels of proinflammatory molecules such as the cytokine IL-6 or the chemokines KC, MCP-1, and MIG were higher in mice with ablated *gly96/iex-1* gene—a condition involving the loss of NF-κB counterregulation by *gly96/iex-1*.[13,18]

While MCP-1 and KC are clearly upregulated during short-term DSS treatment and are associated with acute inflammation, the expression of, i.e., IL-6 and MIG is more pronounced during the course of chronic inflammation, as seen after cyclic 2% DSS treatment for 4 weeks. MCP-1 and KC, both early target genes of NF-κB,[44] are known to be released initially by the damaged intestinal epithelium[45] to attract inflammatory cells such as macrophages and neu trophils.[46] IL-6 and MIG are mainly released by macrophages and are known to stimulate T-cell-dependent immune responses as seen in chronically inflamed colon tissues.

Particularly, MIG has been recently shown to mark the transition from acute to chronic inflammation and to be indispensable for the proinflammatory actions of IFN-γ in CD.[47] Thus, the observed upregulation of this cytokine in gly96/iex-1-deficient mice is in line with the more severe chronic inflammation in these animals and points to the involvement of IFN-γ-dependent pathways in the aggravated inflammatory response. Moreover, gly96/iex-1-deficient mice do not show marked differences in the level of antiinflammatory molecules such as IL-10, indicating that the severe phenotype of DSS-colitis in gly96/iex-1-deficient mice primarily relies on the forced expression of proinflammatory molecules.

The observation that gly96/iex-1 is obviously involved in the control of intestinal immune response fits into the recent notion that gly96/iex-1 is expressed at higher levels in the gut mucosa of inflamed tissue from IBD patients.[34] An explanation might be that gly96/iex-1 is upregulated due to the forced NF-κB induction elicited by an imbalanced immune response. The observed upregulation under inflammatory conditions may thus represent a futile attempt to dampen the NF-κB hyperactivation.[18,48]

As can be appreciated from the results with Pam_3Cys_4-treated BMCs, the functional loss of gly96/iex-1 directly affects the responsiveness of mononuclear cells in terms of NF-κB activation and the release of proinflammatory molecules. Even though lamina propria macrophages differ from BMCs, these findings provide a first mechanistic insight into the proinflammatory effect of gly96/iex-1 deficiency in the colon. Thus, it seems very likely that during the course of DSS-colitis in gly96/iex-1-deficient mice the immune response is much greater due to the lack of NF-κB counterregulation in macrophages, neutrophils, and lymphocytes all involved in IBD at various stages.[5,49] Particularly, the DSS damage induced deterioration of the epithelial barrier function might provoke a much stronger initiation of an inflammatory response in this way, as indicated by the massive elevation of KC and MCP-1 levels in the colon upon short-term DSS treatment. In addition, the decrease of NF-κB counterregulation due to ablation of gly96/iex-1 gene expression may also affect the DSS responsiveness of the colonic epithelia themselves which secrete higher levels of chemokines such as KC and MCP-1, thereby initiating the inflammatory response to DSS treatment more strongly as compared to wildtype *gly96/iex*-1-expressing mice. Since gly96/iex-1 exclusively interacts with p65[13] but not with other NF-κB subunits it does not interfere

with the action of, i.e., p50/p50 homo-dimers, which have been shown to exert antiinflammatory activity.[27,28] Thus, the lack of gly96/iex-1 preferentially augments the proinflammatory potential of NF-κB (namely, by p65/p50), whereas the antiinflammatory actions of NF-κB (namely, by p50/p50) remain unaffected. Moreover, the higher activity of BMCs and the more intense colonic immune response in the absence of gly96/iex-1 favor the view that gyl96/iex-1 has rather proapoptotic than antiapoptotic activity in mononuclear cells that would be otherwise more susceptible to cell death and thereby less inflammatory if gly96/iex-1 had been ablated.

It is also tempting to speculate that gly96/iex-1 deficiency contributes to colorectal carcinogenesis, as one would expect from recent findings.[20–24] The more pronounced chronic inflammation in gly96/iex-1-deficent mice is accompanied by massive alterations in the epithelial architecture—a condition that greatly promotes the formation of preneoplastic lesions.[50] Again, the loss of NF-κB counterregulation by gly96/iex-1 would contribute to inflammation-associated tumorigenesis,[4] presumably involving both deregulation of immune response and higher antiapoptotic protection of the irritated epithelium. It will be interesting to investigate whether somatic genetic alterations in the gly96/iex-1 gene can be found in inflammation-induced tumors that may in turn alter its ability to interfere with NF-κB activity and promote tumorigenesis.

Acknowledgments

The authors thank Ms. Severine Krause for animal care and Ms. Maike Grogßmann for excellent technical assistance.

Supported by the German Research Society (DFG/SFB415-A13, C8) and the German Cluster of Excellence “Inflammation at Interfaces.”

REFERENCES

1. Dutta J, Fan Y, Gupta N, et al. Current insights into the regulation of programmed cell death by NF-kappaB. Oncogene. 2006; 25:6800–6816. [PubMed: 17072329]
2. Ghosh S, Hayden MS. New regulators of NF-kappaB in inflammation. Nat Rev Immunol. 2008; 8:837–848. [PubMed: 18927578]
3. Hayden MS, West AP, Ghosh S. NF-kappaB and the immune response. Oncogene. 2006; 25:6758–6780. [PubMed: 17072327]
4. Karin M, Greten FR. NF-kappaB: linking inflammation and immunity to cancer development and progression. Nat Rev Immunol. 2005; 5:749–759. [PubMed: 16175180]
5. Neurath MF, Pettersson S, Meyer zum Buschenfelde KH, et al. Local administration of antisense phosphorothioate oligonucleotides to the p65 subunit of NF-kappaB abrogates established experimental colitis in mice. Nat Med. 1996; 2:998–1004. [PubMed: 8782457]
6. Schreiber S, Nikolaus S, Hampe J. Activation of nuclear factor kappa B inflammatory bowel disease. Gut. 1998; 42:477–484. [PubMed: 9616307]
7. Rogler G, Brand K, Vogl D, et al. Nuclear factor kappaB is activated in macrophages and epithelial cells of inflamed intestinal mucosa. Gastroenterology. 1998; 115:357–369. [PubMed: 9679041]
8. Perkins ND. Post-translational modifications regulating the activity and function of the nuclear factor kappa B pathway. Oncogene. 2006; 25:6717–6730. [PubMed: 17072324]
9. Hitotsumatsu O, Ahmad RC, Tavares R, et al. The ubiquitin-editing enzyme A20 restricts nucleotide-binding oligomerization domain containing 2-triggered signals. Immunity. 2008; 28:381–390. [PubMed: 18342009]
10. Kondratyev AD, Chung KN, Jung MO. Identification and characterization of a radiation-inducible glycosylated human early response gene. Cancer Res. 1996; 56:1498–1502. [PubMed: 8603392]

11. Pietzsch A, Büchler C, Aslanidis C, et al. Identification and characterization of a novel monocyte/macrophage differentiation-dependent gene that is responsive to lipopolysaccharide, ceramide, and lysophosphatidylcholine. Biochem Biophys Res Commun. 1997; 235:4–9. [PubMed: 9196025]
12. Charles CH, Yoon JK, Simske JS, et al. Genomic structure, cDNA sequence, and expression of gly96, a growth factorinducible immediate-early gene encoding a short-lived glycosylated protein. Oncogene. 1993; 8:797–801. [PubMed: 8437864]
13. Arlt A, Rosenstiel P, Kruse ML, et al. IEX-1 directly interferes with RelA/p65 dependent transactivation and regulation of apoptosis. Biochim Biophys Acta. 2008; 1783:941–952. [PubMed: 18191642]
14. Arlt A, Minkenberg J, Kruse ML, et al. Immediate early gene-X1 interferes with 26 S proteasome activity by attenuating expression of the 19 S proteasomal components S5a/Rpn10 and S1/Rpn2. Biochem J. 2007; 402:367–375. [PubMed: 17107344]
15. Schafer H, Trauzold A, Siegel EG, et al. PRG1: a novel early-response gene transcriptionally induced by pituitary adenylate cyclase activating polypeptide in a pancreatic carcinoma cell line. Cancer Res. 1996; 56:2641–2648. [PubMed: 8653710]
16. Arlt A, Grobe O, Sieke A, et al. Expression of the NF-jB target gene p22PRG1/IEX-1 does not prevent cell death but instead triggers apoptosis in HeLa cells. Oncogene. 2001; 20:69–77. [PubMed: 11244505]
17. Schilling D, Pittelkow MR, Kumar R. IEX-1, an immediate early gene, increases the rate of apoptosis in keratinocytes. Oncogene. 2001; 20:7992–7997. [PubMed: 11753682]
18. Arlt A, Kruse ML, Breitenbroich M, et al. The early response gene IEX-1 attenuates NF-kappaB activation in 293 cells, a possible counter-regulatory process leading to enhanced cell death. Oncogene. 2003; 22:3343–3351. [PubMed: 12761504]
19. Osawa Y, Nagaki M, Banno Y, et al. Expression of the NF-jB target gene IEX-1 enhances TNF-a-induced hepatocyte apoptosis by inhibiting Akt activation. J Immunol. 2003; 170:4053–4060. [PubMed: 12682234]
20. Sebens Muerkoster S, Rausch AV, Isberner A, et al. The apoptosis-inducing effect of gastrin on colorectal cancer cells relates to an increased IEX-1 expression mediating NF-kappa B inhibition. Onco-gene. 2008; 27:1122–1134.
21. Mittal A, Papa S, Franzoso G, et al. NF-kappaB-dependent regulation of the timing of activation-induced cell death of T lymphocytes. J Immunol. 2006; 176:2183–2189. [PubMed: 16455974]
22. Rocher G, Letourneux C, Lenormand P, et al. Inhibition of B56-containing protein phosphatase 2A by the early response gene IEX-1 leads to control of Akt activity. J Biol Chem. 2007; 282:5468–5477. [PubMed: 17200115]
23. Wu MX. Roles of the stress-induced gene IEX-1 in regulation of cell death and oncogenesis. Apoptosis. 2003; 8:11–18. [PubMed: 12510147]
24. Nambiar PR, Nakanishi M, Gupta R, et al. Genetic signatures of high-and low-risk aberrant crypt foci in a mouse model of sporadic colon cancer. Cancer Res. 2004; 64:6394–6401. [PubMed: 15374946]
25. Sasada T, Azuma K, Hirai T, et al. Prognostic significance of the immediate early response gene X-1 (IEX-1) expression in pancreatic cancer. Ann Surg Oncol. 2008; 15:609–617. [PubMed: 18026799]
26. Dilley WG, Kalyanaraman S, Verma S, et al. Global gene expression in neuroendocrine tumors from patients with the MEN1 syndrome. Mol Cancer. 2005; 4:9. [PubMed: 15691381]
27. Oakley F, Mann J, Nailard S, et al. Nuclear factor-kappaB1 (p50) limits the inflammatory and fibrogenic responses to chronic injury. Am J Pathol. 2005; 166:695–708. [PubMed: 15743782]
28. Cao S, Zhang X, Edwards JP, et al. NF-kappaB1 (p50) homodimers differentially regulate pro- and anti-inflammatory cytokines in macrophages. J Biol Chem. 2006; 281:26041–26050. [PubMed: 16835236]
29. Schreiber S, Rosenstiel P, Albrecht M, et al. Genetics of Crohn disease, an archetypal inflammatory barrier disease. Nat Rev Genet. 2005; 6:376–388. [PubMed: 15861209]
30. Podolsky DK. The future of IBD treatment. J Gastroenterol. 2003; 38(suppl 15):63–66.
31. Atreya I, Atreya R, Neurath MF. NF-kappaB in inflammatory bowel disease. J Intern Med. 2008; 263:591–596. [PubMed: 18479258]

32. Nikolaus S, Schreiber S. Diagnostics of inflammatory bowel disease. Gastroenterology. 2007; 133:1670–1689. [PubMed: 17983810]
33. Schulze HA, Hasler R, Mah N, et al. From model cell line to in vivo gene expression: disease-related intestinal gene expression in IBD. Genes Immun. 2008; 9:240–248. [PubMed: 18340362]
34. Costello CM, Mah N, Hasler R, et al. Dissection of the inflammatory bowel disease transcriptome using genome-wide cDNA microarrays. PLoS Med. 2005; 2:e199. [PubMed: 16107186]
35. Elson CO, Sartor RB, Tennyson GS, et al. Experimental models of inflammatory bowel disease. Gastroenterology. 1995; 109:1344–1367. [PubMed: 7557106]
36. Egger B, Bajaj-Elliott M, MacDonald TT, et al. Characterisation of acute murine dextran sodium sulphate colitis: cytokine profile and dose dependency. Digestion. 2000; 62:240–248. [PubMed: 11070407]
37. Byrne FR, Viney JL. Mouse models of inflammatory bowel disease. Curr Opin Drug Discov Dev. 2006; 9:207–217.
38. Sommer SL, Berndt TJ, Frank E, et al. Elevated blood pressure and cardiac hypertrophy after ablation of the gly96/IEX-1 gene. J Appl Physiol. 2006; 100:707–716. [PubMed: 16166241]
39. Becker C, Fantini MC, Wirtz S, et al. In vivo imaging of colitis and colon cancer development in mice using high resolution chromoendoscopy. Gut. 2005; 54:950–954. [PubMed: 15951540]
40. Siegmund B, Lehr HA, Fantuzzi G, et al. IL-1 beta-converting enzyme (caspase-1) in intestinal inflammation. Proc Natl Acad Sci U S A. 2001; 98:13249–13254. [PubMed: 11606779]
41. Muerkoster S, Arlt A, Sipos B, et al. Increased expression of the E3-ubiquitin ligase receptor subunit bTRCP1 relates to constitutive NF-jB activation and chemoresistance in pancreatic carcinoma cells. Cancer Res. 2005; 65:1316–1324. [PubMed: 15735017]
42. Fiocchi C. Inflammatory bowel disease: etiology and pathogenesis. Gastroenterology. 1998; 115:182–205. [PubMed: 9649475]
43. Hanauer SB. Inflammatory bowel disease: epidemiology, pathogenesis, and therapeutic opportunities. Inflamm Bowel Dis. 2006; (suppl 1):S3–9. [PubMed: 16378007]
44. Elewaut D, DiDonato JA, Kim JM, et al. NF-kappa B is a central regulator of the intestinal epithelial cell innate immune response induced by infection with enteroinvasive bacteria. J Immunol. 1999; 163:1457–1466. [PubMed: 10415047]
45. Reinecker HC, Loh EY, Ringler DJ, et al. Monocyte-chemoattractant protein 1 gene expression in intestinal epithelial cells and inflamma-tory bowel disease mucosa. Gastroenterology. 1995; 108:40–50. [PubMed: 7806062]
46. Daig R, Andus T, Aschenbrenner E, et al. Increased interleukin 8 expression in the colon mucosa of patients with inflammatory bowel disease. Gut. 1996; 38:216–222. [PubMed: 8801200]
47. Ito R, Shin-Ya M, Kishida T, et al. Interferon-gamma is causatively involved in experimental inflammatory bowel disease in mice. Clin Exp Immunol. 2006; 146:330–238. [PubMed: 17034586]
48. De Keulenaer GW, Wang Y, Feng Y, et al. Identification of IEX-1 as a biomechanically controlled nuclear factorkappaB target gene that inhibits cardiomyocyte hypertrophy. Circ Res. 2002; 90:690–696. [PubMed: 11934837]
49. Rogler G. Update in inflammatory bowel disease pathogenesis. Curr Opin Gastroenterol. 2004; 20:311–317. [PubMed: 15703658]
50. Itzkowitz SH, Yio X. Inflammation and cancer IV. Colorectal cancer in inflammatory bowel disease: the role of inflammation. Am J Physiol Gastrointest Liver Physiol. 2004; 287:G7–17. [PubMed: 15194558]

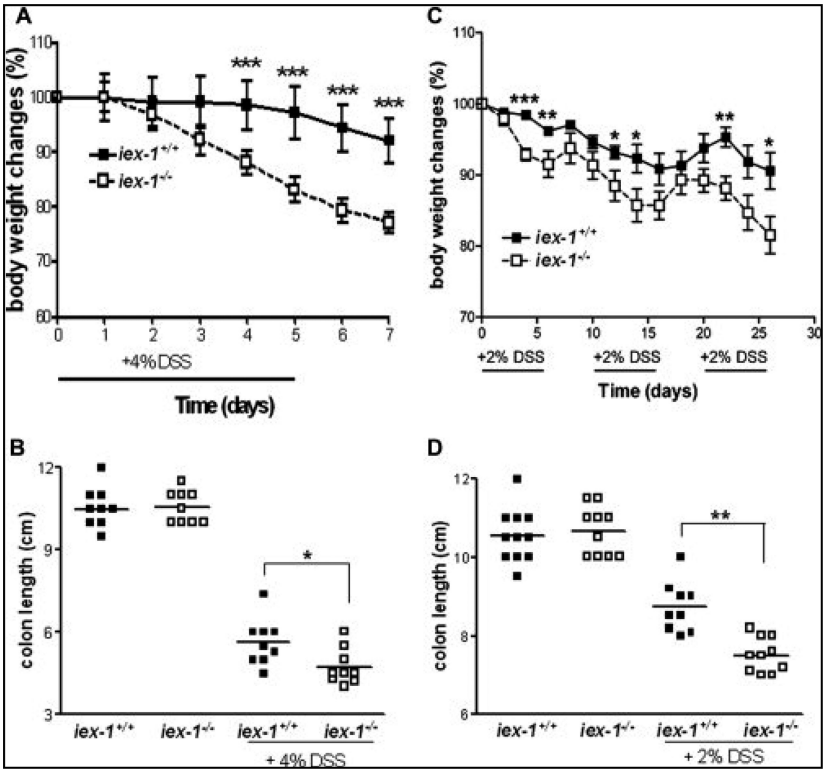

FIGURE 1.

A more severe course of acute and chronic colitis in DSS-treated *gly96/iex-1*$^{-/-}$ mice. *gly96/iex-1*$^{+/+}$ and *gly96/iex-1*$^{-/-}$ mice (male $n = 5$ and female $n = 5$ per each genotype and experiment) were subjected to (A,B) treatment with 4% DSS (p.o.) for 5 days, or (C,D) cyclic treatment with 2% DSS (p.o.) for 4 weeks. Body weight was measured daily (A) or each second day (C) and compared to the initial body weight (data are expressed as mean ± SD of a representative experiment out of 3, *$P < 0.05$, **$P < 0.01$, ***$P < 0.005$). Upon sacrifice on day 7 (B) or day 28 (D), colon lengths were determined (individual data and the median of a representative experiment out of 3 are shown, *$P < 0.05$, **$P < 0.01$).

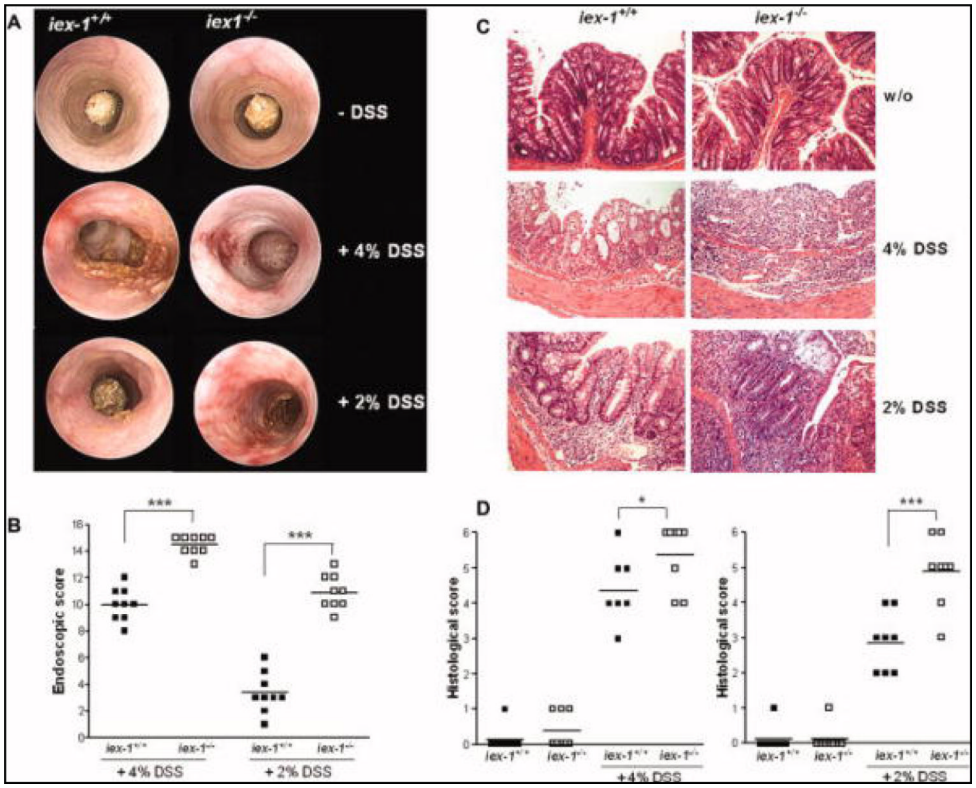

FIGURE 2.

Colon tissue architecture is altered more severely during DSS-induced colitis in *gly96/iex-1*$^{-/-}$ mice. Colonic endoscopy (A) was conducted with untreated *gly96/iex-1*$^{+/+}$ and *gly96/iex-1*$^{-/-}$ mice, with mice treated with 4% DSS for 1 week (coloscopy on day 6, middle panel) and with mice treated with 2% DSS for 4 weeks (coloscopy on day 25, lower panel). Endoscopic scores (B) were determined as previously described[39] (individual data and the median of 1 representative experiment out of 3 are shown, ***$P < 0.005$). Upon sacrifice of control or DSS-treated animals, paraffin-embedded tissue sections from distal colon samples were stained with H&E (C) and visualized at 40× magnification (representative images are shown). Histological scores (D) were determined as previously reported[40] (individual data and the median of a representative experi ment out of 3 are shown; *$P < 0.05$, ***$P <$ 0.005).

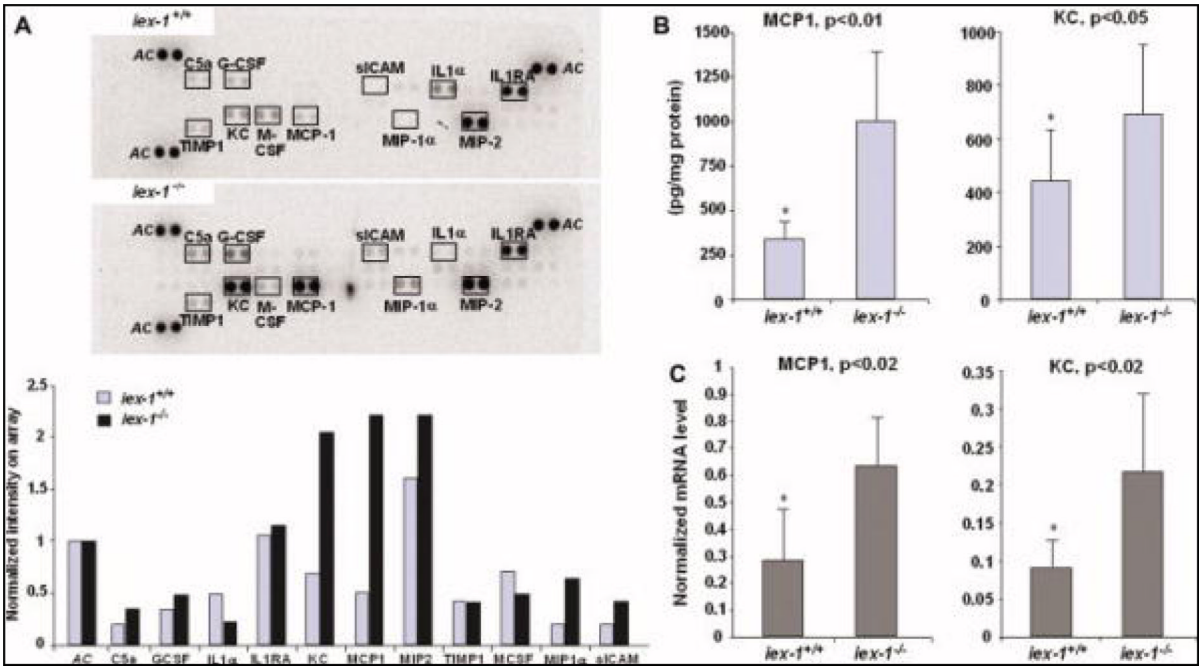

FIGURE 3.

Enhanced expression of proinflammatory chemo/cytokines in *gly96/iex-1*$^{-/-}$ mice during acute DSS colitis. Supernatants of colon tissue kept in culture for 24 hours from 4% DSS-treated *gly96/iex-1*$^{+/+}$ and *gly96/iex-1*$^{-/-}$ mice were analyzed (A) using proteome profiler arrays detecting a broad panel of murine chemo- and cytokines. Densitometry (lower panel) of the developed arrays (upper panel) was conducted to normalize signal intensities to internal array controls (AC) and for comparison between *gly96/iex-1*$^{+/+}$ and *gly96/iex-1*$^{-/-}$ mice. ELISA assays (B) were conducted on the supernatants from cultured colonic tissue to quantify the secretion of MCP-1 and KC in *gly96/iex-1*$^{+/+}$ and *gly96/iex-1*$^{-/-}$ mice (data represent the mean ± SD from 3 independent experiments). Total RNA from colonic tissues was submitted to reverse transcription and subsequent qPCR (C) using specific primers detecting MCP-1 and KC or β-actin as a control. The MCP-1 and KC mRNA levels were calculated after normalization to β-actin mRNA (data represent the mean ± SD from 3 independent experiments). [Color figure can be viewed in the online issue, which is available at www.interscience.wiley.com.]

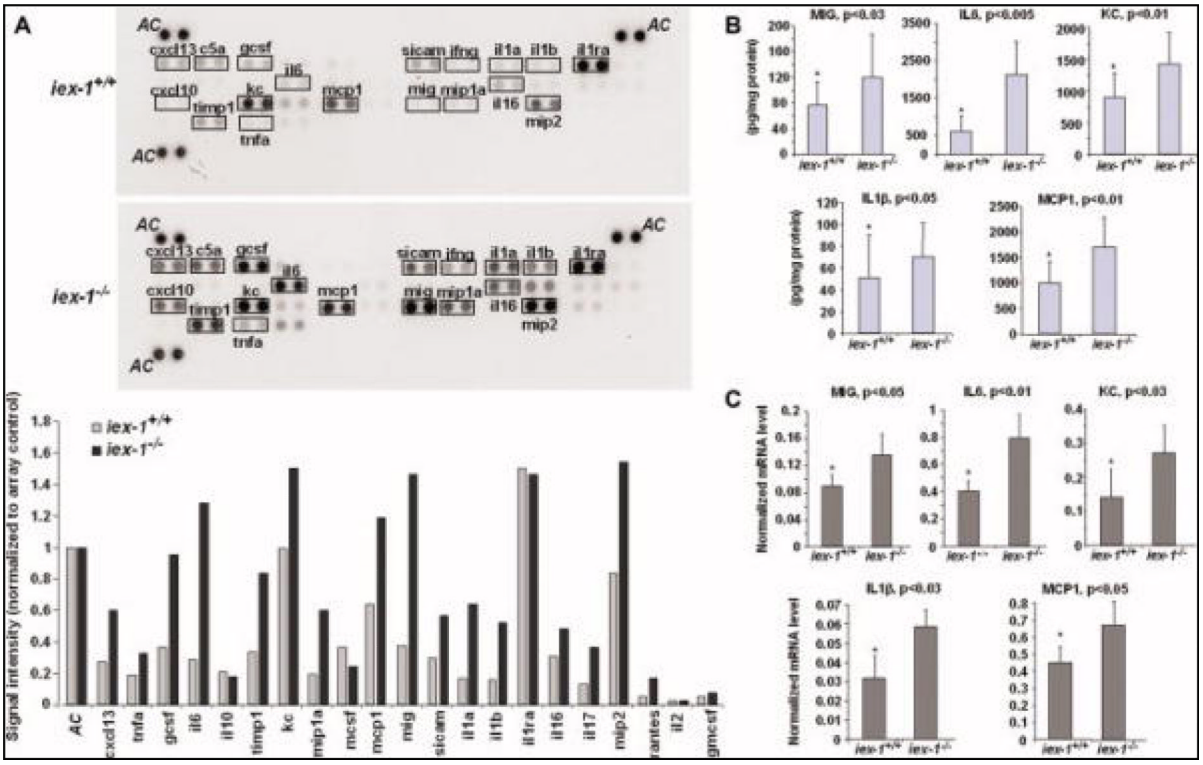

FIGURE 4.

Enhanced expression of proinflammatory chemo/cytokines in *gly96/iex-1*$^{-/-}$ mice during chronic DSS colitis. Supernatants of colon tissue kept in culture for 24 hours from 2% DSS-treated *gly96/iex-1*$^{+/+}$ and *gly96/iex-1*$^{-/-}$ mice were analyzed (A) using proteome profiler arrays detecting a broad panel of murine chemo- and cytokines. Densitometry (lower panel) of the developed arrays (upper panel) was conducted to normalize signal intensities to internal array controls (AC) and for comparison between *gly96/iex-1*$^{+/+}$ and *gly96/iex-1*$^{-/-}$ mice. ELISA assays (B) were conducted on the supernatants from cultured colonic tissue to quantify the secretion of MCP-1, KC, IL-6, IL-1*β*, and MIG in *gly96/iex-1*$^{+/+}$ and *gly96/iex-1*$^{-/-}$ mice (data represent the mean ± SD of 3 independent experiments). Total RNA from colonic tissues was submitted to reverse transcription and subsequent qPCR (C) using specific primers detecting MCP-1, KC, IL-6, IL-1*β*, and MIG or *β*-actin as a control. The cyto- and chemokine mRNA levels were calculated after normalization to *β*-actin mRNA (data represent the mean ± SD of 3 independent experiments). [Color figure can be viewed in the online issue, which is available at www.interscience.wiley.com.]

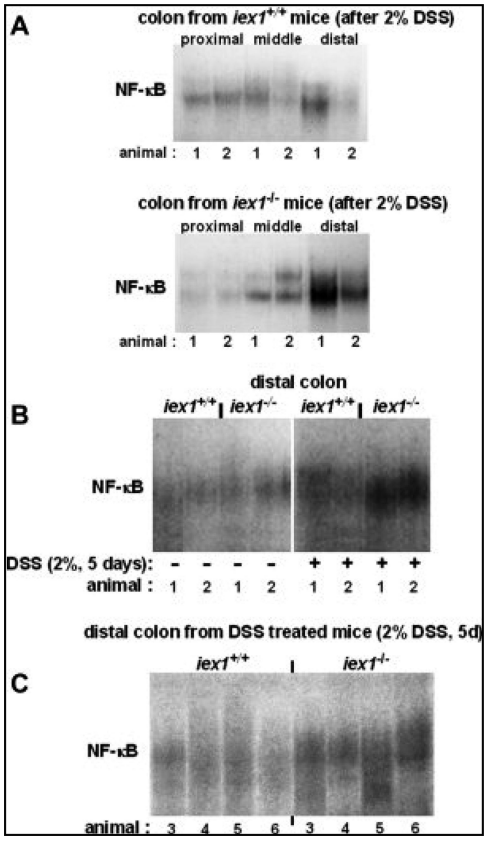

FIGURE 5.

Increased NF-κB activation in the distal colon of *gly96/iex-1*$^{-/-}$ mice during chronic DSS colitis. Colon tissue samples from 2% DSS (5 days) treated *gly96/iex-1*$^{+/+}$ and *gly96/iex-1*$^{-/-}$ mice were used for the preparation of nuclear extracts and subsequent gel shift assays for the detection of NF-κB activity. (A) Distinct segments of the colon from either 2 (animals 1, 2) DSS-treated *gly96/iex-1*$^{+/+}$ and *gly96/iex-1*$^{-/-}$ mice were analyzed. (B) Distal colon samples from 2 untreated and 2 DSS-treated *gly96/iex-1*$^{+/+}$ and *gly96/iex-1*$^{-/-}$ mice were analyzed. (C) Distal colon samples from 4 additional DSS-treated *gly96/iex-1*$^{+/+}$ or *gly96/iex-1*$^{-/-}$ mice were analyzed.

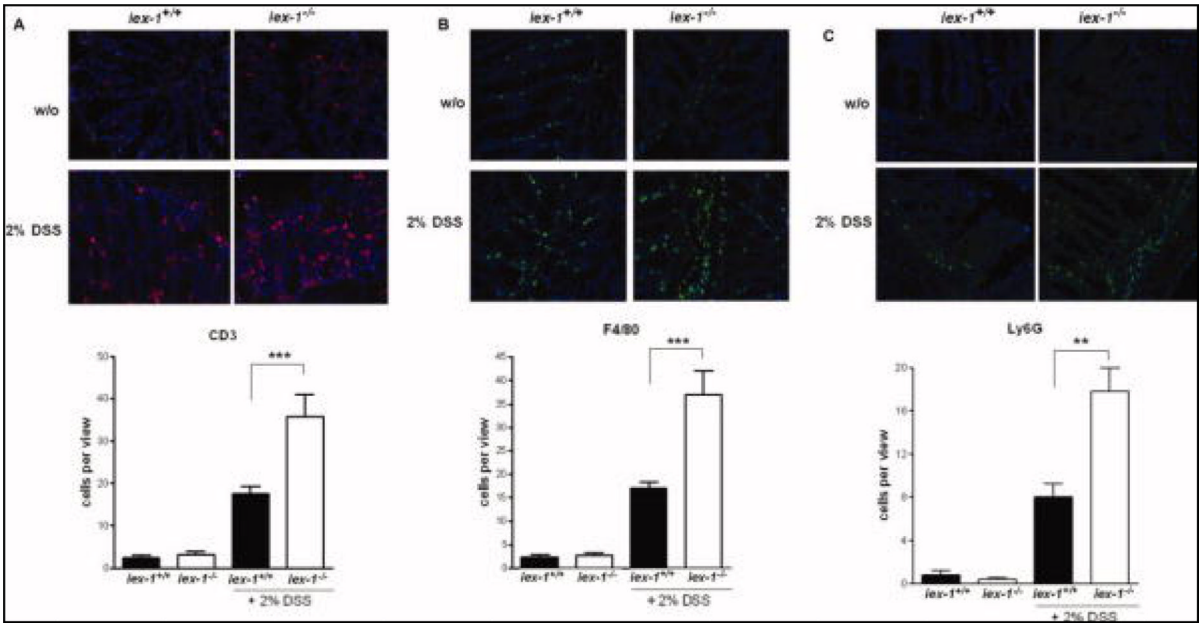

FIGURE 6.

Increased leukocyte infiltrations in the colonic mucosa of DSS-treated *gly96/iex-1*$^{-/-}$ mice. Colon tissue samples from 2% DSS-treated *gly96/iex-1*$^{+/+}$ and *gly96/iex-1*$^{-/-}$ mice were used for anti-CD3, anti-F4/80, and anti-Ly6G immunofluorescence microscopy for the detection of T-lymphocytes (A), tissue macrophage and monocytes (B), and neutrophils (C). A 40 magnification was used to visualize CD3, F4/80, and Ly6G immunofluorescence staining. Four representative microscopic fields of all tissue sections ($n = 8$) were evaluated for the corresponding positivity count per view (mean ± SD; $^{**}P < 0.01$, $^{***}P < 0.005$).

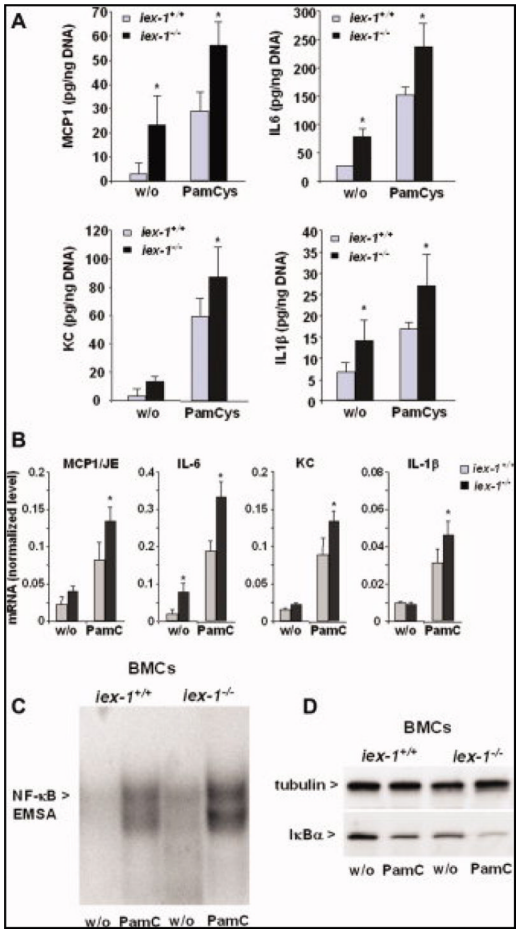

FIGURE 7.

Induction of proinflammatory chemo/cytokines and activation of NF-κB is greater in BMCs from *gly96/iex-1*$^{-/-}$ than in BMCs from *gly96/iex-1*$^{+/+}$ mice. Supernatants (A) of BMCs from *gly96/iex-1*$^{+/+}$ and *gly96/iex-1*$^{-/-}$ mice kept in culture for 72 hours and then subjected to Pam_3Cys_4 treatment (200 ng/mL) for 24 hours or not were submitted to ELISA detecting MCP-1, IL-6, KC, and IL-1β (data represent the mean ± SD of 4 independent experiments, *$P < 0.05$). Total RNA (B) of BMCs from *gly96/iex-1*$^{+/+}$ and *gly96/iex-1*$^{-/-}$ mice kept in culture for 72 hours and then subjected to Pam_3Cys_4 treatment (200 ng/mL, 4 h) or not was submitted to reverse transcription and subsequent qPCR detecting MCP-1, IL-6, KC, and IL-1β or β-actin as control. The cyto- and chemokine mRNA levels were calculated after normalization to β-actin mRNA (data represent the mean ± SD of 4 independent experiments, *$P < 0.05$). Nuclear extracts (C) from untreated or Pam_3Cys_4 treated (200 ng/mL, 1 h) BMCs were submitted to gel shift assay for the detection of NF-κB; a representative experiment out of 3 is shown. (D) Cytoplasmic extracts from untreated or Pam_3Cys_4 treated (200 ng/mL, 30 min) BMCs were submitted to an anti-IκBα Western blot, and tubulin was detected as a Western blot loading control. A representative experiment out of 3 is shown. [Color figure can be viewed in the online issue, which is available at www.interscience.wiley.com.]